

PRECIOUS METAL COMPLEXES OF SOME
NOVEL FUNCTIONALISED SECONDARY
AND TERTIARY PHOSPHINES

by

Joanne H Downing

A thesis submitted to the University of Bristol in accordance with the requirements for
the degree of Doctor of Philosophy in the School of Chemistry, Faculty of Science.

November 1992

CHAPTER 3

METAL COMPLEXES OF THE CAGE SECONDARY PHOSPHINE 1,3,5,7-TETRAMETHYL-2,4,8- TRIOXA-6-PHOSPHAADAMANTANE

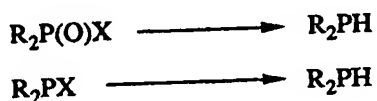
3.1 Introduction

The co-ordination chemistry of secondary phosphines is much less well studied than that of tertiary phosphines.⁴⁵ We were particularly interested in secondary phosphines as ligands to co-ordinatively unsaturated d⁸ metals because of their role in hydrophosphination reactions as a route to poly(tertiary)phosphines (Chapter 4). The corresponding tertiary phosphine area is a vast one in comparison.⁴⁵⁻⁴⁷

3.1.1 Synthesis of Secondary Phosphines

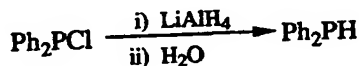
A. By Reduction of other Phosphorus Compounds

This is the most widely used method of synthesis of secondary phosphines.⁴⁸



Equation 3.1

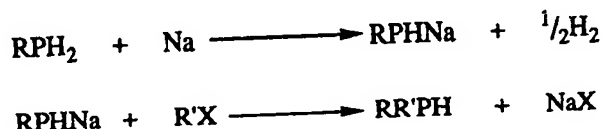
The X group is usually a halide, but may also be OR,⁴⁹ SR⁵⁰ or OH⁵¹ (Equation 3.1). The most common reducing agent is lithium aluminium hydride.⁵²⁻⁵⁴ A simple example is the reduction of chlorodiphenylphosphine with an excess of LiAlH₄ followed by hydrolysis to afford diphenylphosphine⁵⁵ (Equation 3.2).



Equation 3.2

B. From Metal Phosphides

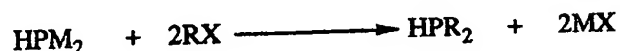
The reaction of one equivalent of an alkali metal with a primary phosphine generates a mono-metallated phosphide^{56,57} (Equation 3.3). Subsequent treatment of the phosphide with an organohalide affords a symmetrical or unsymmetrical secondary phosphine depending on the organohalide used.^{58,59}



Equation 3.3

In this way phenylphosphine is converted to the unsymmetrical ethylphenylphosphine.⁵⁸

Symmetrical secondary phosphines can be derived from dimetallated phosphides and an alkylhalide⁵⁹ (Equation 3.4).

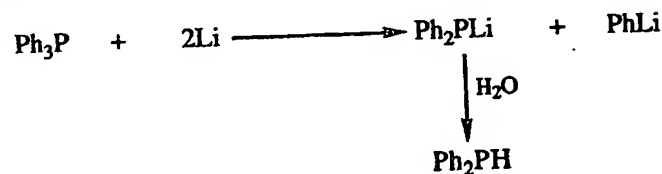


Equation 3.4

In general the synthesis of dimetallated derivatives of phosphine is difficult and yields of secondary phosphine by this route are low.

C. By P-C Bond Cleavage

Treatment of tertiary phosphines with an alkali metal may result in P-C bond cleavage, subsequent treatment with water affords a secondary phosphine.^{60,61} This method can be successfully employed to produce diphenylphosphine from triphenylphosphine⁶¹ (Equation 3.5).



Equation 3.5

Recently sonication has been found to assist P-C bond cleavage with lithium.⁶²

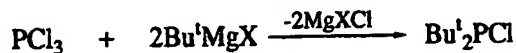
D. From Elemental Phosphorus

It is sometimes possible to synthesise phosphines directly from red or white phosphorus.⁶³ This usually requires high temperatures and pressures and yields are low. For example, the interaction of phenyllithium or phenylmagnesium bromide with elemental phosphorus gives low yields (15%) of diphenylphosphine.⁶⁴

E. By Reaction of a Grignard with Phosphorus Halides

The reaction of phosphorus trichloride with a Grignard reagent usually results in substitution of all the halogen atoms and so is a convenient route to tertiary phosphines.⁴⁸ With bulky substituents less substituted products may result, for

example the reaction of t-butylmagnesium halide with phosphorus trichloride (Equation 3.6).

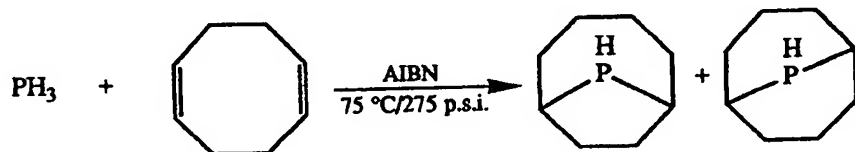


Equation 3.6

The chloro group can then be reduced to give the secondary phosphine di-t-butylphosphine.⁶⁵

F. From Phosphine

The addition of phosphine to multiple bonds is one of the most economical ways of making phosphines.⁴⁸ If the multiple bond is activated by electron withdrawing groups the P-H addition may occur at elevated temperatures.^{66,67} However, a catalyst is usually required; this can be an acid,⁶⁸⁻⁷² a base,^{73,74} a transition metal complex⁷⁵⁻⁷⁷ or a radical initiator^{34,78-80} and the multiple bond can be an olefin,^{34,73,74,77-80} acetylene,⁸¹⁻⁸³ a carbonyl group^{71,72,75,76} or an isocyanate.^{84,85} Thus by varying the catalyst, the unsaturated species and the reaction conditions a wide variety of phosphines is accessible by this route.⁴⁸ In practice it is often difficult to stop the addition of all three of the P-H bonds of phosphine and isolation of secondary phosphines is not always easy. The free radical initiated addition of phosphine to 1,5-cyclooctadiene is one example where the addition stops at the secondary phosphine³⁴ (Equation 3.7). A 63% yield of bis(2-cyanoethyl)phosphine can be achieved by the slow addition of acrylonitrile to a solution kept saturated with phosphine⁷³ (Equation 3.8).

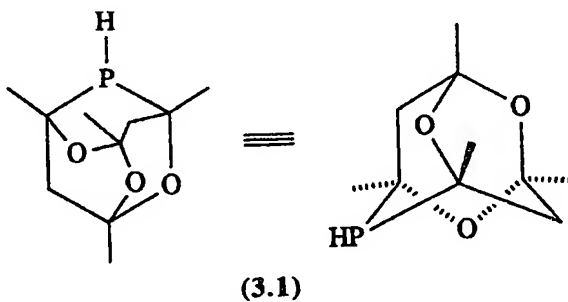


Equation 3.7



Equation 3.8

Another case where it is very easy to isolate a secondary phosphine is the acid catalysed addition of phosphine to 2,4-pentanedione.⁸⁶ Epstein *et al*⁸⁶ found that solutions of 2,4-pentanedione in aqueous hydrochloric acid absorbed phosphine readily and a crystalline white solid was precipitated. They ascertained that this was a secondary phosphine by a combination of spectroscopic and chemical techniques. The infrared spectrum of the product exhibited a single P-H absorption at 2280 cm⁻¹ and the proton coupled ³¹P NMR spectrum showed a 1:1 doublet. The chemical properties of the product were typical of a secondary phosphine; reactions such as oxidation and quaternisation were successful. All this information together with elemental analysis and ¹H NMR led Epstein and Buckler⁸⁶ to propose that the product of the reaction of 2,4-pentanedione with phosphine was 1,3,5,7-tetramethyl-2,4,8-trioxa-6-phosphadamantane (3.1).

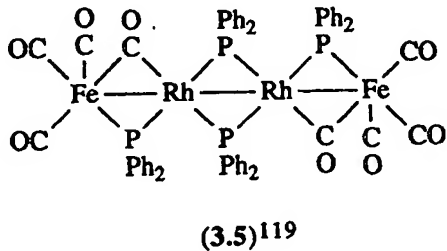
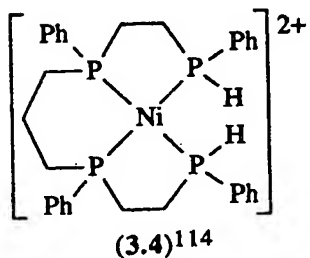
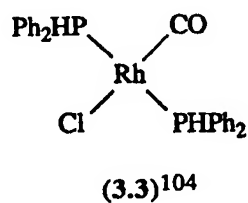
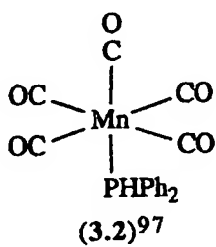


The phosphine (3.1) could be readily isolated in an 80% yield. There was no spectroscopic evidence for any tertiary phosphine addition products. The remaining P-H bond is unreactive towards further addition presumably for steric reasons. The unusual cage secondary phosphine (3.1) was found to be relatively unreactive towards atmospheric oxygen in the solid state and in solution compared to simpler dialkyl secondary phosphines and it has no unpleasant odour. So not only is it easy to prepare and easy to isolate but also easy to handle.

3.1.2 Transition Metal Complexes of Secondary Phosphines

Tertiary phosphines are among the most widely used ligands in transition metal chemistry.⁴⁵⁻⁴⁷ They have found extensive use in homogeneous catalysis (*e.g.* hydroformylation,⁸⁷ hydrogenation,^{88,89} hydroamination,⁹⁰ hydrosilylation,⁹¹ olefin metathesis⁸⁹ and carbon-carbon bond formation⁹²). Secondary phosphine transition metal complexes are comparatively under studied. This is most likely due to the ease with which their P-H bonds cleave on reaction with a metal centre to give phosphido bridged metal complexes.⁹³ The area has not however been totally neglected and

complexes are known for a variety of transition metals (e.g. V,⁹⁴ Cr,⁹⁵ Mo,⁹⁶ Mn,⁹⁷ Ru,⁹⁸⁻¹⁰¹ Os,¹⁰¹ Co,^{102,103} Rh,^{100,104,105} Ir,¹⁰⁰ Ni,^{97,100,106-109} Pd,^{100,108,109} Pt,^{100,108,109} Ag,¹¹⁰ Au,¹¹¹ Cd¹¹² and Hg^{112,113}).

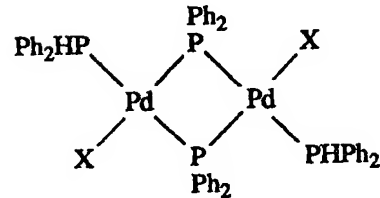
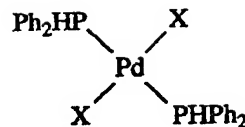


The study of co-ordinated secondary phosphines is attractive for a number of reasons. The P-H bonds may be susceptible to a variety of chemical transformations. For example, they may act as precursors to multidentate phosphorus ligands¹¹⁴⁻¹¹⁸ or to polynuclear phosphido bridged species^{104,119-122} such as (3.5). The presence of the P-H bond leads to easy spectroscopic study.

We were interested in metal complexes in which the P-H bond remains intact, particularly those of co-ordinatively unsaturated platinum(II) and palladium(II), where oxidative addition reactions are commonplace.⁶ Secondary phosphine complexes are used in the metal template synthesis of multidentate phosphorus ligands (Chapter 4). The earliest reports indicating the complexity of the reactions of secondary phosphines with metal halides were by Issleib and co-workers.^{123,124} They showed that diphenylphosphine did not always remain intact on reaction with a metal.

3.1.2.1 Palladium(II) Complexes

In 1962 Hayter¹²⁵ carried out reactions of diphenylphosphine with palladium dihalides with a view to forming compounds of the type $[\text{PdX}_2(\text{PHPh}_2)_2]$ [(3.6) X = Cl; (3.7) X = Br; (3.8) X = I]. He was unable to isolate the palladium complex (3.6) due to the ease of elimination of HCl. Instead the phosphido bridged complex (3.9) was isolated.

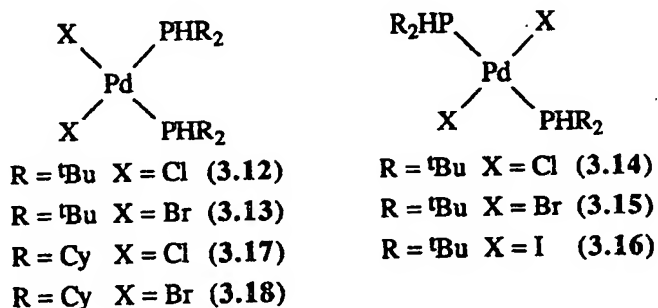


However, from the reaction of diphenylphosphine with palladium dibromide it is possible to isolate the mononuclear dibromopalladium(II) complex (3.7) but only in low yields as the phosphido bridged complex (3.10) also forms. In fact, if the same reaction is carried out in methanol the phosphido bridged complex (3.10) is the sole product. In contrast the reaction of diphenylphosphine with palladium diiodide affords the mononuclear secondary phosphine complex (3.8) in 70% yield and there is no evidence for the formation of the phosphido bridged complex (3.11). Hayter¹²⁵ concluded that the elimination of HX from $[\text{PdX}_2(\text{PPh}_2)_2]$ is easiest for $\text{X} = \text{Cl}$ and hardest for $\text{X} = \text{I}$.

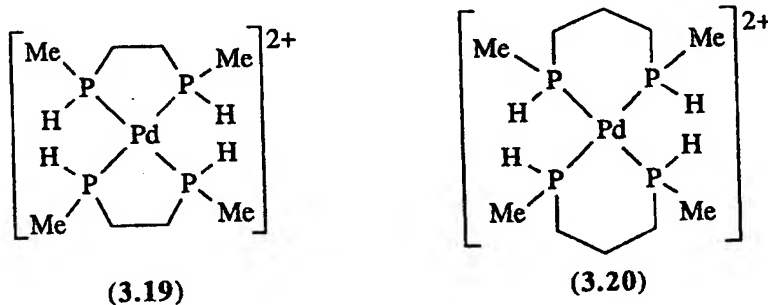
In later work Hayter^{126,127} does however isolate dichloropalladium(II) complexes of diethylphosphine, dimethylphosphine and ethylphenylphosphine. The lower acidity of dialkyl and alkylarylphosphines than diphenylphosphine is probably the explanation for the increased stability of their metal complexes with respect to deprotonation.¹²⁶ The dibromo and diiodo palladium(II) complexes of diethylphosphine have also been prepared and readily isolated. Elimination of HX, as with the analogous dichloropalladium(II) complex, occurs only in the presence of a base.

Shaw *et al*¹⁰⁰ produced a series of compounds of di-*t*-butylphosphine including *cis*- $[\text{PdCl}_2(\text{PH}^t\text{Bu}_2)_2]$ (3.12), *cis*- $[\text{PdBr}_2(\text{PH}^t\text{Bu}_2)_2]$ (3.13) and their *trans* isomers, (3.14) and (3.15), and *trans*- $[\text{PdI}_2(\text{PH}^t\text{Bu}_2)_2]$ (3.16) with a view to studying their proton NMR spectra in detail. These dialkylphosphine palladium complexes show no

tendency to form phosphido complexes. Similarly,¹²⁸ the complexes *cis*-[PdX₂(PHCy₂)₂] [(3.17) X = Cl; (3.18) X = Br] are stable in the absence of base.



More recently,¹¹⁷ the secondary phosphine palladium(II) complexes (3.19) and (3.20) have been prepared for their use in the template synthesis of macrocyclic phosphorus ligands.

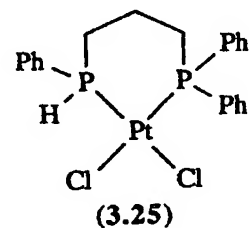
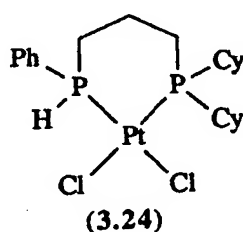


3.1.2.2 Platinum(II) Complexes

Similar attempts have been carried out to prepare platinum(II) complexes of diphenylphosphine.¹²⁹ It was not possible to isolate complexes of the type [PtX₂(PPh₂)₂] even for X = Br and X = I and the phosphido bridged dimers [{PtX(μ-PPh₂)(PPh₂)₂}]₂ [(3.21) X = Cl; (3.22) X = Br; (3.23) X = I] were isolated instead. A comparison with the analogous palladium(II) chemistry indicates that deprotonation of the secondary phosphine occurs more readily for the platinum(II) complexes. It is likely that the formation of a phosphido complex from a secondary phosphine involves oxidative addition of the P-H bond to give a metal hydride species as an intermediate, with subsequent elimination of HX.¹²⁹ It is well known¹³⁰ that Pt-H bonds are more stable than Pd-H bonds; this may result in more facile P-H bond cleavage in the platinum case.

Levason and co-workers¹²⁹ conclude that the synthesis of secondary phosphine complexes of platinum(II) would appear to be very difficult and in fact examples are

even less common than for palladium(II). Using the bulky di-*t*-butylphosphine Shaw *et al.*¹⁰⁰ isolated the compounds *cis*- and *trans*-[PtX₂(PH^tBu₂)₂] [X = Cl, Br, I] and more recently,¹³¹ bidentate secondary-tertiary phosphines have been used to form [PtCl₂(L-L)] [(3.24) L-L = PhHP(CH₂)₃PCy₂; (3.25) L-L = PhHP(CH₂)₃PPh₂].



3.1.3 Aims of the Present Work

The co-ordination chemistry of secondary phosphines with d⁸ co-ordinatively unsaturated metals has been comparatively little studied. Dialkylphosphines offer the best chance of obviating the formation of phosphido bridged products. We aimed to study the co-ordination chemistry of the unusual fused tricyclic secondary phosphine 1,3,5,7-tetramethyl-2,4,8-trioxa-6-phosphaadamantane (3.1), in particular with platinum(II) and palladium(II). This dialkyl secondary phosphine (3.1) is readily synthesised from phosphine and 2,4-pentanedione. It is easy to isolate and easy to handle, being an air stable crystalline solid.

3.2 Synthesis and Characterisation of 1,3,5,7-Tetramethyl-2,4,8-trioxa-6-Phosphaadamantane

Epstein and Buckler⁸⁶ isolated the secondary phosphine (3.1) from the reaction of phosphine and 2,4-pentanedione in aqueous hydrochloric acid in a pressure bottle with shaking at 2-3 atmospheres for 50 min. We found that the same reaction could be carried out at atmospheric pressure although the reaction time was increased to 7 hours. Phosphine gas was bubbled through a solution of 2,4-pentanedione in aqueous hydrochloric acid and the temperature was raised to between 40 °C and 50 °C. After 7 hours the uptake of phosphine was negligible and a white solid had precipitated. This was readily isolated by filtration in air.

The proton coupled phosphorus NMR data reported by Epstein⁸⁶ were a doublet at $\delta(^{31}P) -51.5$ p.p.m., we observed a doublet of multiplets [$\delta(^{31}P) -49.5$ p.p.m., $^{1}J(PH) 189.6$ Hz] (Figure 3.1). From our analysis of the proton NMR spectrum (see later), the phosphorus is coupled not only to the P-H proton but also to two inequivalent sets of methyl protons and three of the four inequivalent methylene

protons; some of these smaller couplings are clearly being observed in the proton coupled ^{31}P NMR spectrum.

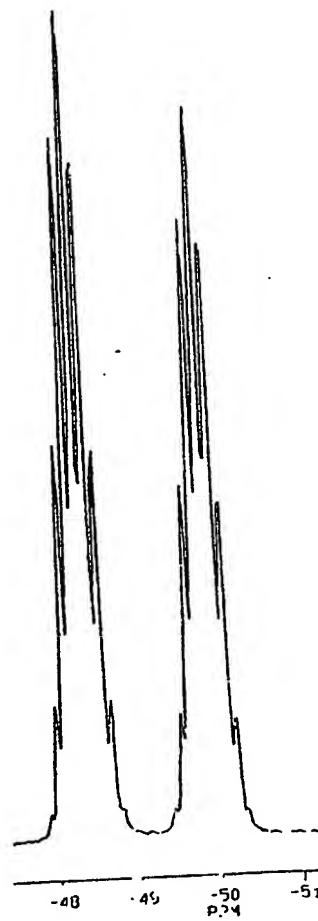


Figure 3.1 Proton coupled ^{31}P NMR spectrum of the secondary phosphine (3.1).

No $^{13}\text{C}({}^1\text{H})$ NMR data were reported by Epstein *et al.*⁸⁶ The $^{13}\text{C}({}^1\text{H})$ NMR spectrum shown in Figure 3.2 shows ten individual signals were observed which reflects the lack of symmetry in the secondary phosphine (3.1) (Figure 3.3). In order to distinguish carbon-phosphorus coupling from distinct carbon signals the spectrum was recorded at both 100 MHz and 67.5 MHz. The $^{13}\text{C}({}^1\text{H})$ NMR data are reported in Table 3.1.

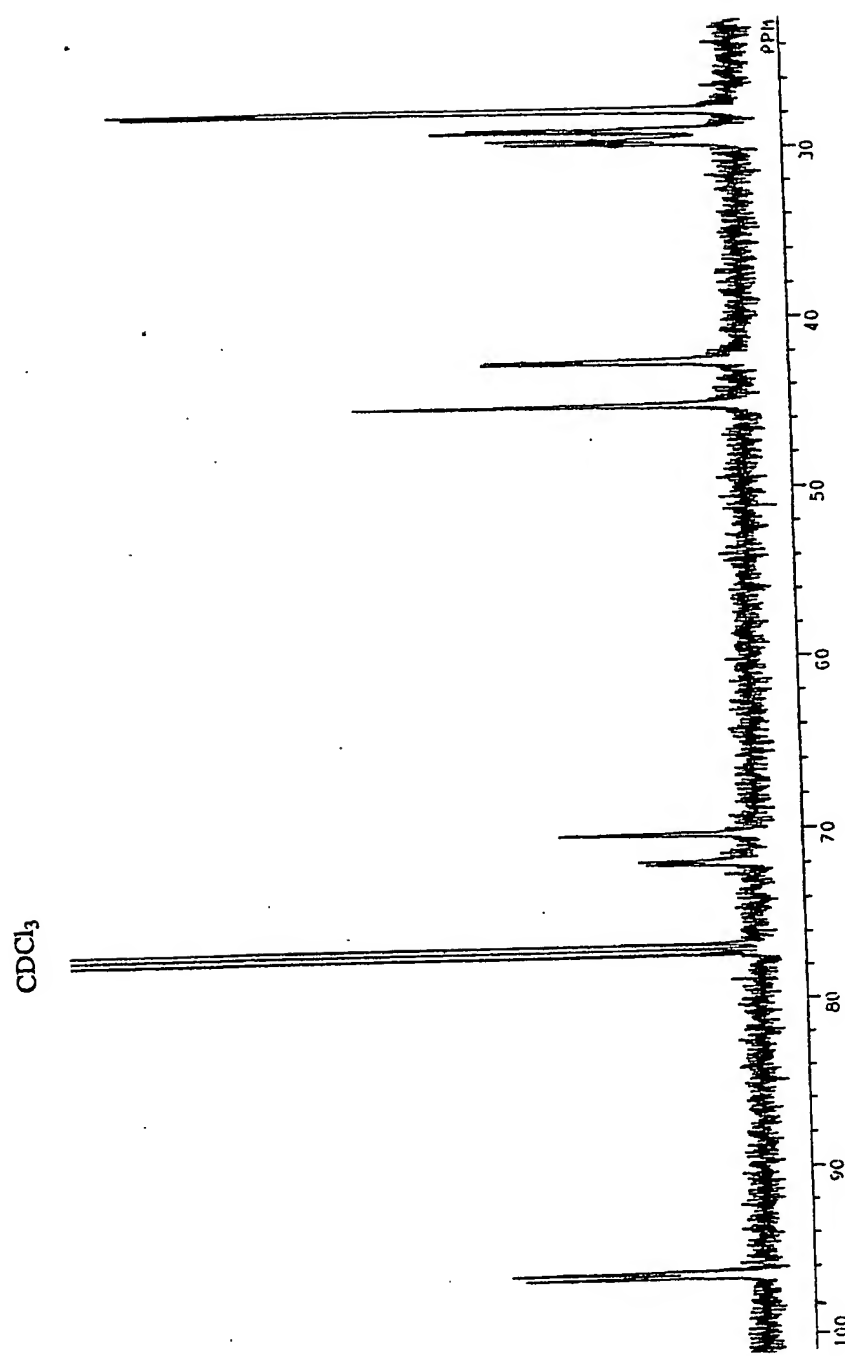


Figure 3.2 $^{13}\text{C}\{^1\text{H}\}$ NMR spectrum for the secondary phosphine (3.1).

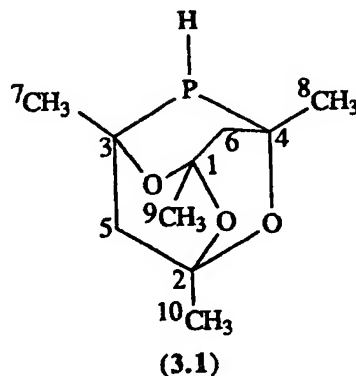


Figure 3.3 The number of signals expected in the $^{13}\text{C}\{^1\text{H}\}$ NMR spectrum of (3.1).

Table 3.1 $^{13}\text{C}\{^1\text{H}\}$ NMR^a data for the cage secondary phosphine (3.1).

Carbon atom number ^b	$\delta(^{13}\text{C})$	$nJ(\text{PC})$
1	96.6	-c
2	96.3	-c
3	71.9	18.3 (n = 1)
4	70.3	-c
5	45.1	-c
6	45.6	13.8 (n = 2)
7	29.7	22.9 (n = 2)
8	29.0	12.2 (n = 2)
9	27.9	-c
10	27.7	-c

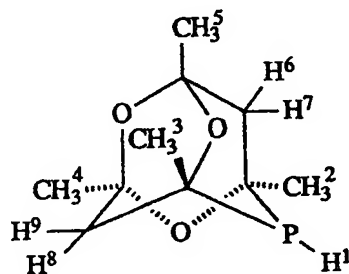
^a Spectra (100 MHz) measured in CDCl_3 at 20 °C. Chemical shifts [$\delta(^{13}\text{C})$] in p.p.m. (± 0.1) to high frequency of tetramethylsilane. Coupling constants in Hz (± 0.1).

^b Numbering scheme according to Figure 3.3.

^c $nJ(\text{PC})$ not observed.

The ^1H NMR spectral data were reported by Epstein and Buckler⁸⁶ but they were not able to conclude any more than the presence of methyl, methylene and P-H protons in the correct ratio for their proposed structure. We remeasured the spectrum which is shown in Figure 3.4. The lack of symmetry in the P-H signal was curious and full analysis of the spectrum required a 2D COSY NMR spectrum (Figures 3.5a and 3.5b) and simulation of the methylene region (Figures 3.6a and 3.6b). The derived data for (3.1) are reported in Table 3.2.

Table 3.2 ^1H NMR^a data for the secondary phosphine (3.1).



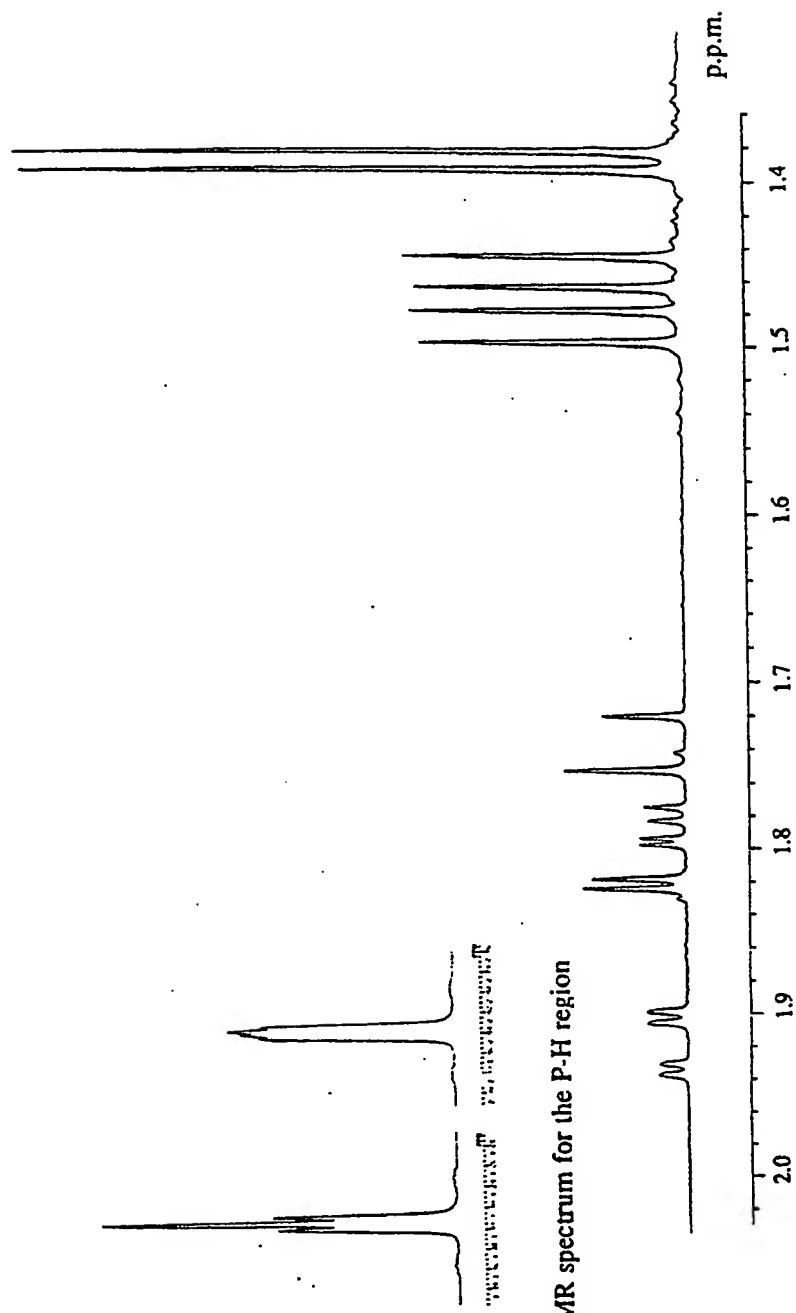
Proton atom number ^b	$\delta(^1\text{H})$	$^nJ(\text{PH})$
1 ^d	3.08	189.6 (n = 1)
2	1.48	13.7 (n = 3)
3	1.46	13.6 (n = 3)
4	1.39	-c
5	1.38	-c
6 ^e	1.73	-c
7 ^f	1.91	2.6 (n = 3)
8 ^g	1.79	21.4 (n = 3)
9 ^h	1.81	6.6 (n = 3)

^a Spectrum (400 MHz) measured in CDCl_3 at 20 °C. Chemical shifts [$\delta(^1\text{H})$] in p.p.m. (± 0.01) to high frequency of tetramethylsilane. Coupling constants in Hz (± 0.1). ^b Numbering scheme according to diagram. ^c $^nJ(\text{PC})$ not observed.

^d $4J(\text{H}^1\text{H}^9)$ 1.6 Hz; $4J(\text{H}^1\text{H}^8)$ 3.2 Hz; $4J(\text{H}^1\text{H}^7)$ 0.6 Hz. ^e $2J(\text{H}^6\text{H}^7)$ 12.8 Hz.

^f $4J(\text{H}^1\text{H}^7)$ 0.6 Hz; $2J(\text{H}^6\text{H}^7)$ 12.8 Hz. ^g $4J(\text{H}^1\text{H}^8)$ 3.2 Hz; $2J(\text{H}^8\text{H}^9)$ 13.1 Hz.

^h $4J(\text{H}^1\text{H}^9)$ 1.6 Hz; $2J(\text{H}^8\text{H}^9)$ 13.1 Hz.



^1H NMR spectrum for the P-H region

Figure 3.4 ^1H NMR spectrum for the secondary phosphine (3.1).

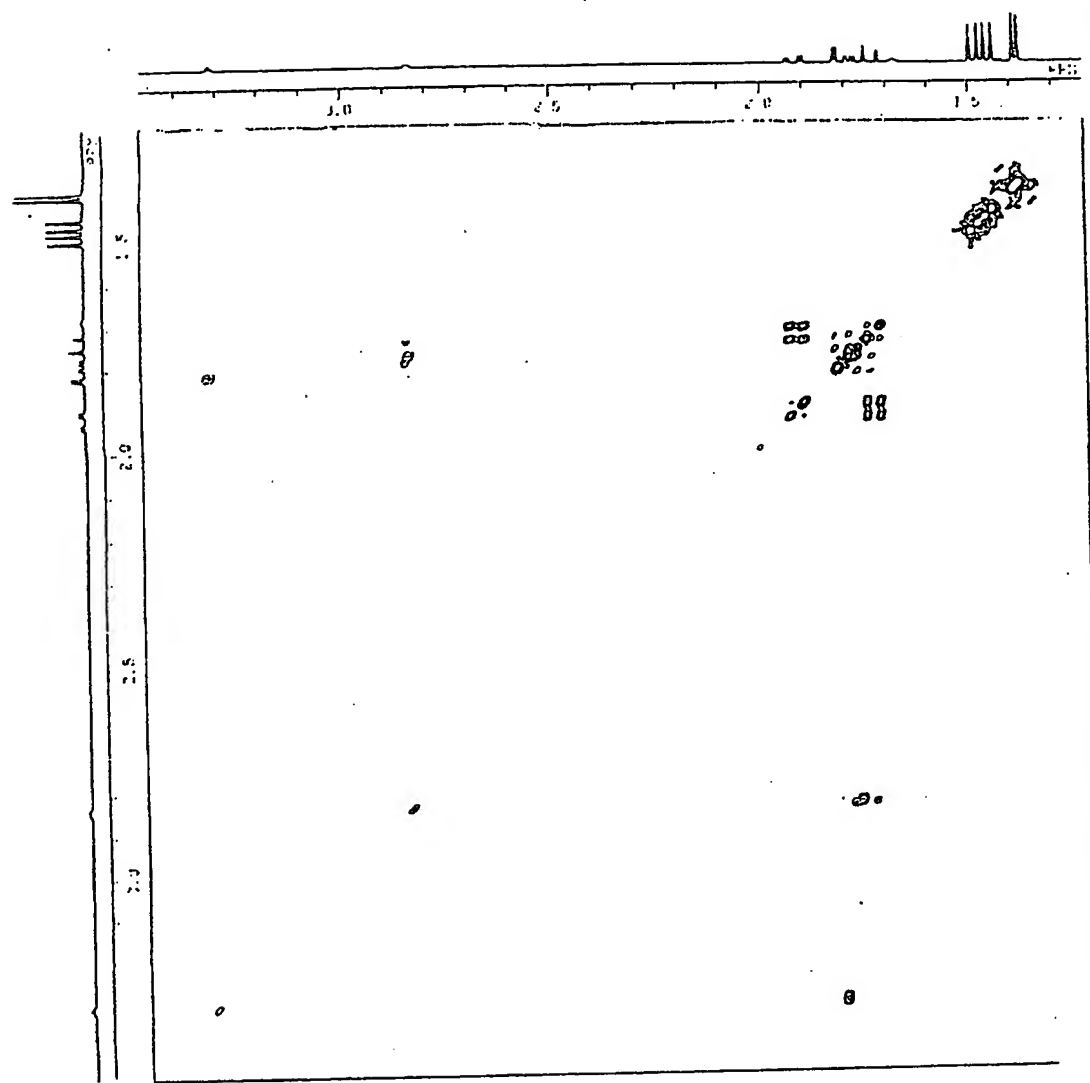


Figure 3.5a 2D COSY NMR spectrum of (3.1).

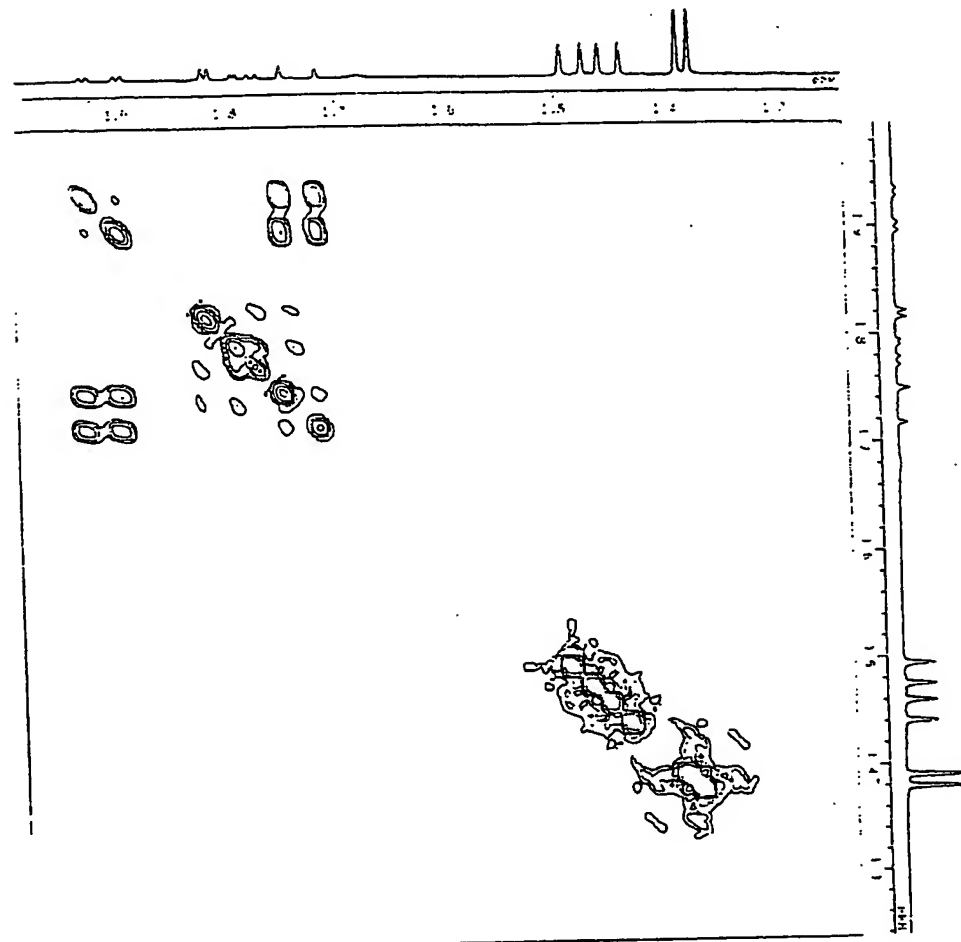


Figure 3.5b Expansion of the methylene region of the 2D COSY NMR spectrum of (3.1)

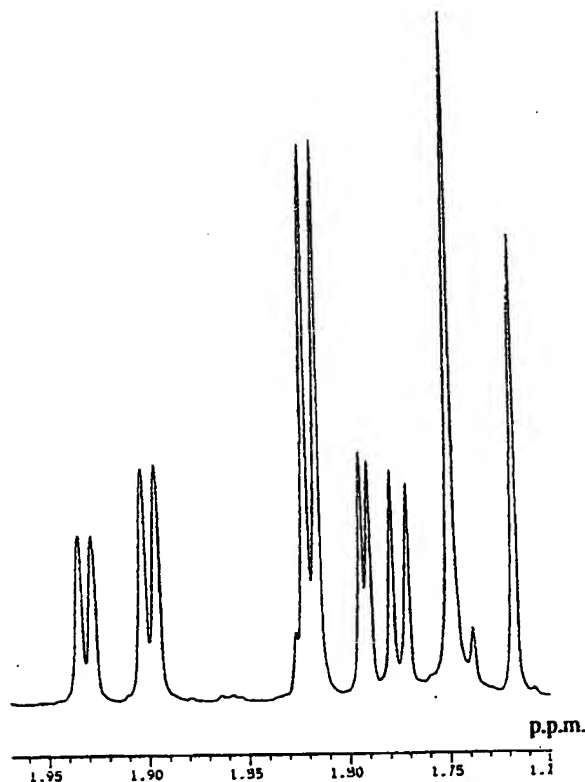


Figure 3.6a Expansion of the methylene region of the ¹H NMR spectrum of (3.1).

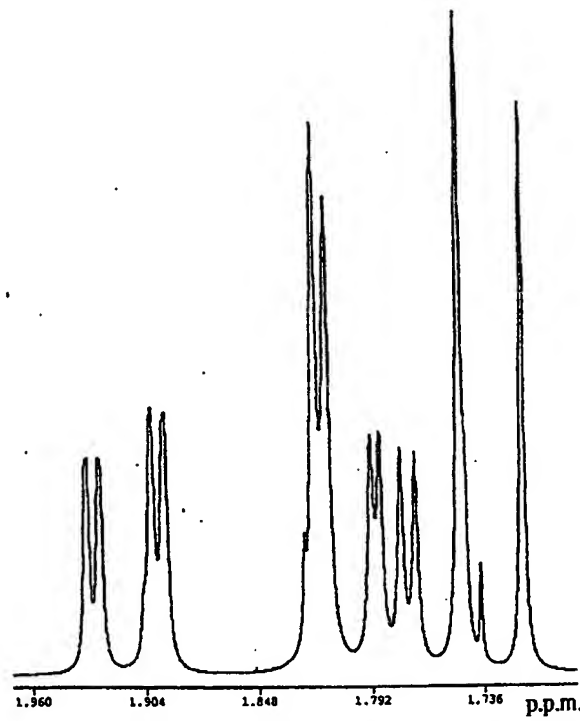
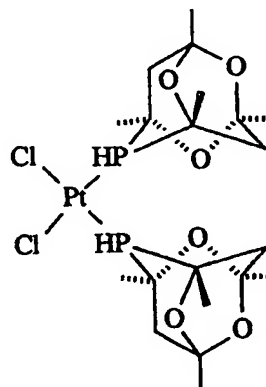


Figure 3.6b Simulation of the methylene region of the ¹H NMR spectrum of (3.1).

This novel cage phosphine is soluble in common organic solvents and air stable compared to other dialkyl secondary phosphines.

3.3 Platinum(II) Complexes of 1,3,5,7-Tetramethyl-2,4,8-trioxa-6-Phosphaadamantane

Addition of two equivalents of the secondary phosphine (3.1) to $[\text{PtCl}_2(\text{cod})]$ in dichloromethane resulted in precipitation of a white solid which was only sparingly soluble in common solvents (e.g. dichloromethane, chloroform, acetone and methanol). The complex was assigned the structure *cis*- $[\text{PtCl}_2(\text{adamphos})_2]$ [(3.26), adamphos = (3.1)] following characterisation by $^{31}\text{P}\{^1\text{H}\}$ and proton coupled ^{31}P NMR spectroscopy (Table 3.3), elemental analysis (Experimental) and X-ray crystallography (Section 3.4.1).



cis- $[\text{PtCl}_2(\text{adamphos})_2]$ (3.26)

The $^{31}\text{P}\{^1\text{H}\}$ NMR spectrum shows a singlet with ^{195}Pt satellites [$\delta(^{31}\text{P})$ 0.3 p.p.m., $^1J(\text{PtP})$ 3301 Hz] (Table 3.3); presumably the two diastereomers expected, due to the phosphine existing in two enantiomeric forms, have coincident chemical shifts. In the proton coupled ^{31}P NMR spectrum we would expect to see an AA'XX' pattern, the doublet observed is characteristic of *cis* complexes in which $^2J(\text{PP}')$ is small and the separation of the two signals is $^1J(\text{PH}) + ^3J(\text{PH})$. The phosphorus-proton coupling (405 Hz) is greatly increased from that of the free phosphine (189.6 Hz) which is typical of such complexes¹²⁸ (e.g. *cis*- $[\text{PdCl}_2(\text{PHC}_2\text{H}_5)_2]$ 345 Hz). This is indicative of an increase in s character of the P-H bond upon co-ordination to a metal. The broadness of the proton coupled spectrum can be ascribed to unresolved couplings of the phosphorus to the methyl and methylene protons.

The addition of an excess of lithium bromide or lithium iodide to the isolated dichloroplatinum(II) complex (3.26) led to the formation of the corresponding dibromo (3.27) and diiodo (3.28) complexes. These were characterised by $^{31}\text{P}\{^1\text{H}\}$ NMR spectroscopy (Table 3.3) and elemental analysis (Experimental).

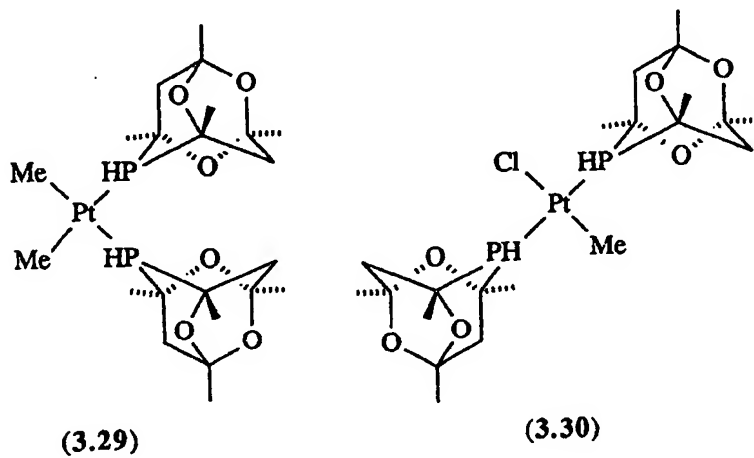
Table 3.3 $^{31}\text{P}\{^1\text{H}\}$ NMR^a data for some platinum(II) complexes of (3.1).

Complex		$\delta(^{31}\text{P})$	$^1J(\text{PtP})$	$^{11}J(\text{PH}) + ^3J(\text{PH})$
<i>cis</i> -[PtCl ₂ (adamphos) ₂]	(3.26)	0.3	3301	405
<i>cis</i> -[PtBr ₂ (adamphos) ₂]	(3.27)	5.2	3237	372
<i>cis</i> -[PtI ₂ (adamphos) ₂]	(3.28)	7.3	3101	361
<i>cis</i> -[PtMe ₂ (adamphos) ₂]	(3.29)	10.5	1790	-
<i>trans</i> -[Pt(Me)Cl(adamphos) ₂] ^b	(3.30)	9.4	2193	369
		9.2	2193	369

^a Spectra (36.2 MHz) measured in CDCl_3 at 28 °C. Chemical shifts [$\delta(^{31}\text{P})$] in p.p.m. (± 0.1) to high frequency of 85% H_3PO_4 . Coupling constants in Hz (± 3).

^b Two signals observed due to the presence of diastereomers.

The reaction of two equivalents of the secondary phosphine (3.1) with [PtMe₂(cod)] was studied by $^{31}\text{P}\{^1\text{H}\}$ NMR spectroscopy (Table 3.3). The species formed initially showed a broad singlet with ^{195}Pt satellites [$^1J(\text{PtP})$ 1790 Hz] which was assigned to the expected dimethylplatinum(II) complex (3.29). After 12 hours in solution the $^{31}\text{P}\{^1\text{H}\}$ NMR spectrum showed two sharp singlets in approximately 1:1 ratio, tentatively assigned to diastereomers of the *trans* methyl(chloro)platinum(II) complex (3.30), most likely resulting from the reaction of the dimethyl complex with the chlorinated solvent in which the reaction was carried out.



3.4 X-ray Crystal Structure Study of Two Secondary Phosphine Platinum(II) Complexes

3.4.1 X-ray Crystal Structure of $[\text{PtCl}_2(\text{adamphos})_2]$ (3.26)

Crystals of $[\text{PtCl}_2(\text{adamphos})_2]$ (3.26) were obtained from a dichloromethane / diethyl ether solution and the crystal structure was determined by R.D. Jackson in this department. The complex was found to crystallise as discrete molecules in the monoclinic space group Cc with one molecule of dichloromethane per unit cell co-crystallised. Bond lengths and angles (numbering scheme shown in Figure 3.7) are listed in Tables 3.4 and 3.5.

The geometry around the platinum is essentially square planar with two ligands (3.1) and two chlorine atoms in a *cis* arrangement about the platinum. As Figure 3.7 shows the phosphines arrange themselves such that the adamantyl cages are as far apart as possible, leaving the protons pointing towards each other. This is the expected orientation on steric grounds.

Table 3.4 Bond lengths (\AA) for the dichloroplatinum complex (3.26).

Atoms	Bond lengths (\AA)	Atoms	Bond lengths (\AA)
Pt-P(1)	2.232 (3)	Pt-P(2)	2.274 (5)
Pt-Cl(1)	2.309 (5)	Pt-Cl(2)	2.352 (4)
P(1)-C(11)	1.859 (12)	P(1)-C(16)	1.848 (15)
P(2)-C(21)	1.878 (13)	P(2)-C(26)	1.878 (16)
O(1)-C(13)	1.423 (18)	O(1)-C(16)	1.428 (21)
O(3)-C(13)	1.427 (20)	O(3)-C(18)	1.447 (28)
O(2)-C(11)	1.468 (16)	O(2)-C(18)	1.422 (21)
C(10)-C(11)	1.543 (22)	C(11)-C(12)	1.495 (26)
C(12)-C(13)	1.505 (22)	C(13)-C(14)	1.508 (35)
C(15)-C(16)	1.508 (21)	C(16)-C(17)	1.536 (21)
C(17)-C(18)	1.468 (26)	C(18)-C(19)	1.525 (27)
O(4)-C(21)	1.451 (14)	O(4)-C(28)	1.409 (18)
O(5)-C(23)	1.453 (22)	O(5)-C(26)	1.412 (24)
O(6)-C(23)	1.416 (22)	O(6)-C(28)	1.435 (23)
C(20)-C(21)	1.485 (22)	C(21)-C(22)	1.515 (29)
C(22)-C(23)	1.513 (29)	C(23)-C(24)	1.489 (42)
C(25)-C(26)	1.496 (20)	C(26)-C(27)	1.536 (20)
C(27)-C(28)	1.528 (18)	C(28)-C(29)	1.502 (20)
Cl(3)-C(3)	1.749 (22)	Cl(4)-C(3)	1.737 (22)

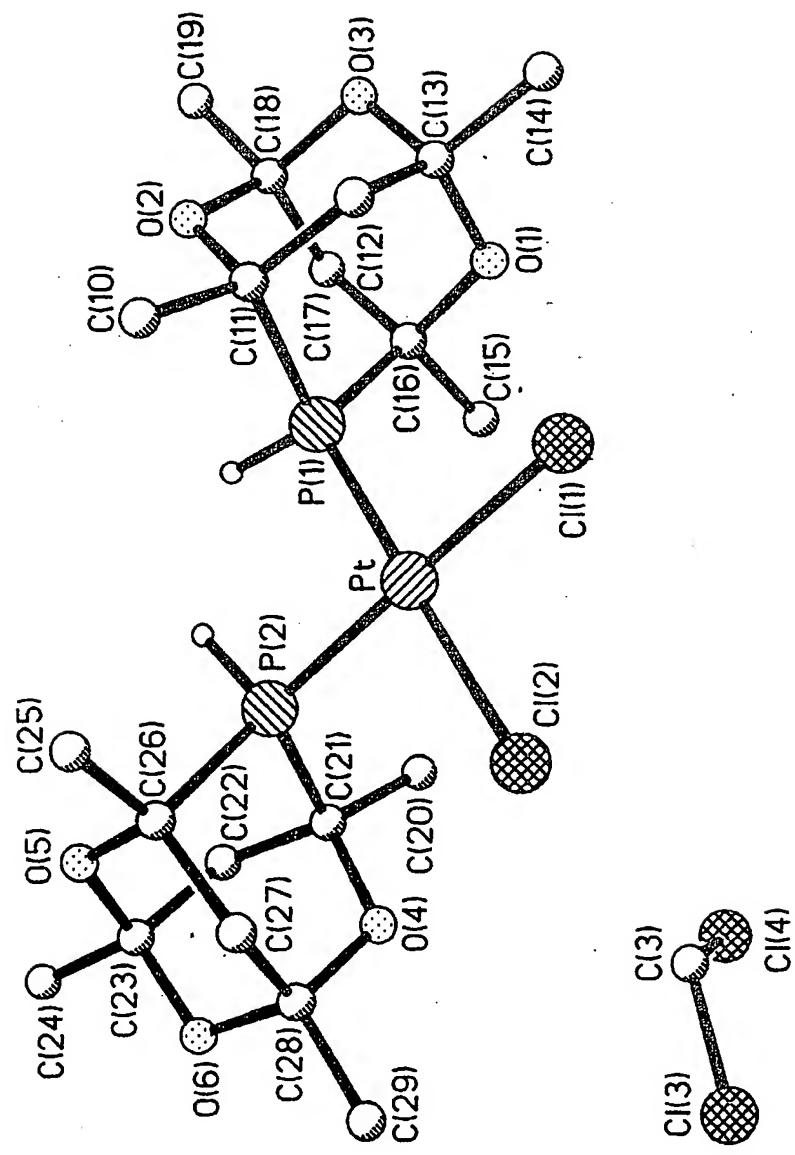


Figure 3.7 A view of the molecular structure of the dichloroplatinum(II) complex (3.26) showing the numbering scheme. Hydrogen atoms are omitted for clarity.

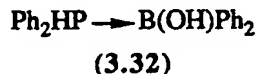
Table 3.5 Bond angles ($^{\circ}$) for the dichloroplatinum complex (3.26).

Atoms	Angles ($^{\circ}$)	Atoms	Angles ($^{\circ}$)
P(1)-Pt-P(2)	88.1(1)	P(1)-Pt-Cl(1)	92.1(1)
P(2)-Pt-Cl(1)	179.3(1)	P(1)-Pt-Cl(2)	177.8(1)
P(2)-Pt-Cl(2)	91.6(2)	Cl(1)-Pt-Cl(2)	88.3(2)
Pt-P(1)-C(11)	122.0(4)	Pt-P(1)-C(16)	117.5(5)
C(11)-P(1)-C(16)	95.0(7)	Pt-P(2)-C(21)	118.9(6)
Pt-P(2)-C(26)	123.4(5)	C(21)-P(2)-C(26)	95.2(6)
C(13)-O(1)-C(16)	115.5(13)	C(13)-O(3)-C(18)	109.7(13)
C(11)-O(2)-C(18)	114.2(13)	P(1)-C(11)-O(2)	105.6(8)
P(1)-C(11)-C(10)	109.9(10)	O(2)-C(11)-C(10)	107.1(13)
P(1)-C(11)-C(12)	109.5(10)	O(2)-C(11)-C(12)	108.9(11)
C(10)-C(11)-C(12)	115.3(12)	C(11)-C(12)-C(13)	111.5(12)
O(1)-C(13)-O(3)	110.1(12)	O(1)-C(13)-C(12)	113.3(13)
O(3)-C(13)-C(12)	107.1(15)	O(1)-C(13)-C(14)	105.6(16)
O(3)-C(13)-C(14)	107.7(14)	C(12)-C(13)-C(14)	112.9(14)
P(1)-C(16)-O(1)	109.6(8)	P(1)-C(16)-C(15)	112.8(10)
O(1)-C(16)-C(15)	106.4(14)	P(1)-C(16)-C(17)	107.5(11)
O(1)-C(16)-C(17)	108.8(12)	C(15)-C(16)-C(17)	111.7(12)
C(16)-C(17)-C(18)	109.2(12)	O(3)-C(18)-O(2)	111.6(13)
O(3)-C(18)-C(17)	109.1(17)	O(2)-C(18)-C(17)	113.0(15)
O(3)-C(18)-C(19)	105.6(17)	O(2)-C(18)-C(19)	105.4(17)
C(17)-C(18)-C(19)	111.9(14)	C(21)-O(4)-C(28)	116.8(11)
C(23)-O(5)-C(26)	117.7(16)	C(23)-O(6)-C(28)	112.9(14)
P(2)-C(21)-O(4)	107.4(8)	P(2)-C(21)-C(20)	111.4(10)
O(4)-C(21)-C(20)	107.5(12)	P(2)-C(21)-C(22)	106.2(10)
O(4)-C(21)-C(22)	109.3(12)	C(20)-C(21)-C(22)	114.9(12)
C(21)-C(22)-C(23)	112.3(14)	O(5)-C(23)-O(6)	110.6(14)
O(5)-C(23)-C(22)	108.3(16)	O(6)-C(23)-C(22)	108.0(18)
O(5)-C(23)-C(24)	108.8(19)	O(6)-C(23)-C(24)	109.3(17)
C(22)-C(23)-C(24)	111.9(17)	P(2)-C(26)-O(5)	106.9(9)
P(2)-C(26)-C(25)	110.4(11)	O(5)-C(26)-C(25)	108.3(16)
P(2)-C(26)-C(27)	106.3(12)	O(5)-C(26)-C(27)	110.7(12)
C(25)-C(26)-C(27)	114.0(12)	C(26)-C(27)-C(28)	110.2(11)
O(4)-C(28)-O(6)	110.5(10)	O(4)-C(28)-C(27)	111.1(12)
O(6)-C(28)-C(27)	108.2(13)	O(4)-C(28)-C(29)	107.5(13)
O(6)-C(28)-C(29)	107.2(13)	C(27)-C(28)-C(29)	112.4(11)
Cl(3)-C(3)-Cl(4)	112.2(11)		

3.4.2 Synthesis and X-ray Crystal Structure of $[\text{PtCl}_2(\text{PPh}_2\text{H})_2]$ (3.31)

The complex *cis*- $[\text{PtCl}_2(\text{PPh}_2\text{H})_2]$ (3.31) was prepared by a somewhat circuitous route. A direct synthesis from diphenylphosphine and $[\text{PtCl}_2(\text{cod})]$ was investigated but it proved impossible to prevent the reaction from proceeding to phosphido bridged complexes. Levason *et al.*¹²⁹ had previously tried reacting diphenylphosphine with $[\text{PtCl}_2(\text{PhCN})_2]$ and were only able to isolate the binuclear phosphido bridged complex (3.21). It has been established^{125,126,129} that secondary phosphine complexes of the type $[\text{MX}_2(\text{PhR}_2)_2]$ are most likely to undergo HX elimination when $\text{M} = \text{Pt}$, $\text{X} = \text{Cl}$ and $\text{R} = \text{Ph}$. So it is not surprising that the complex (3.31) has remained elusive.

We have previously prepared a boron stabilised adduct of diphenylphosphine (3.32) which is an insoluble air stable white solid. Two equivalents of (3.32) were stirred with $[\text{PtCl}_2(\text{cod})]$ over twelve hours to give a clear solution from which was isolated *cis*- $[\text{PtCl}_2(\text{PPh}_2\text{H})_2]$ (3.31) (see Experimental for $^{31}\text{P}\{^1\text{H}\}$ NMR data). The ease of isolation of the product in this case is tentatively attributed to the ease of weighing out 2 equivalents of the solid form of diphenylphosphine and the slow release of diphenylphosphine from the boron adduct.



Colourless crystals of (3.31) were grown from dichloromethane / pentane and the crystal structure was determined by S. Shaw and R.D. Jackson in this department. The complex was found to crystallise as discrete molecules in the monoclinic space group $P2_1/c$. Bond lengths and angles are listed in Tables 3.6 and 3.7 using the numbering scheme shown in Figure 3.8. The P-H protons were located in the fourier difference map and refined successfully.

The geometry around the platinum is essentially square planar with two diphenylphosphine moieties and two chlorine atoms in a *cis* arrangement about the platinum. As Figure 3.8 shows the phosphines arrange themselves such that the P-H protons point towards each other. This is again the expected orientation on steric grounds.

Table 3.6 Bond lengths (\AA) for the dichloroplatinum(II) complex (3.31).

Atoms	Bond lengths (\AA)	Atoms	Bond lengths (\AA)
Pt-Cl(1)	2.361 (4)	Pt-Cl(2)	2.370 (3)
Pt-P(1)	2.221 (3)	Pt-P(2)	2.230 (4)
P(1)-C(11)	1.777 (14)	P(1)-C(21)	1.811 (14)
P(2)-C(31)	1.818 (12)	P(2)-C(41)	1.775 (15)
C(11)-C(12)	1.332 (21)	C(11)-C(16)	1.389 (22)
C(12)-C(13)	1.399 (36)	C(13)-C(14)	1.350 (33)
C(14)-C(15)	1.375 (28)	C(15)-C(16)	1.404 (33)
C(31)-C(32)	1.389 (17)	C(31)-C(36)	1.357 (17)
C(32)-C(33)	1.360 (19)	C(33)-C(34)	1.357 (21)
C(34)-C(35)	1.376 (23)	C(35)-C(36)	1.374 (23)
C(41)-C(42)	1.395 (23)	C(41)-C(46)	1.365 (23)
C(42)-C(43)	1.441 (33)	C(43)-C(44)	1.341 (30)
C(44)-C(45)	1.347 (33)	C(45)-C(46)	1.365 (37)
C(21)-C(26)	1.299 (21)	C(21)-C(22)	1.331 (26)
C(26)-C(25)	1.380 (28)	C(25)-C(24)	1.209 (32)
C(24)-C(23)	1.282 (33)	C(22)-C(23)	1.371 (38)

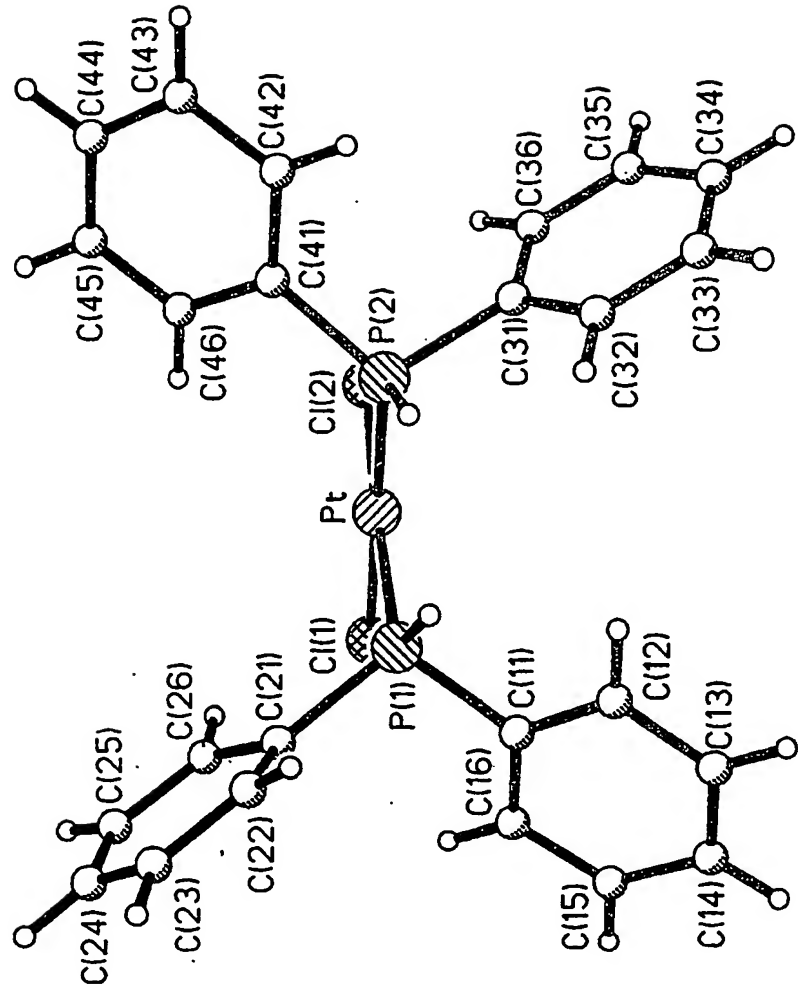


Figure 3.8 A view of the molecular structure of the dichloroplatinum(II) complex (3.31) showing the numbering scheme. Hydrogen atoms are omitted for clarity.

Table 3.7 Bond angles (°) for the dichloroplatinum(II) complex (3.31).

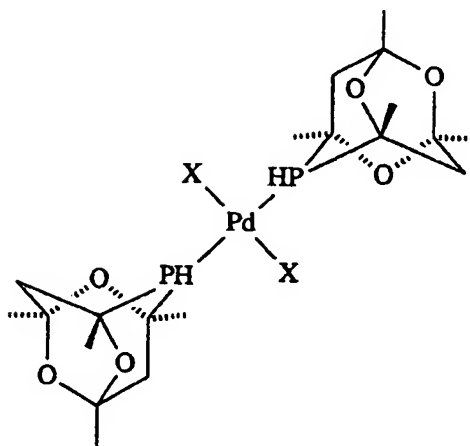
Atoms	Bond Angles (°)	Atoms	Bond Angles (°)
Cl(1)-Pt-Cl(2)	90.5(1)	Cl(1)-Pt-P(1)	88.5(1)
Cl(2)-Pt-P(1)	177.3(1)	Cl(1)-Pt-P(2)	179.0(1)
Cl(2)-Pt-P(2)	88.6(1)	P(1)-Pt-P(2)	92.5(1)
Pt-P(1)-C(11)	116.2(4)	Pt-P(1)-C(21)	116.6(4)
C(11)-P(1)-C(21)	107.1(6)	Pt-P(2)-C(31)	115.5(4)
Pt-P(2)-C(41)	115.6(5)	C(31)-P(2)-C(41)	107.9(6)
P(1)-C(11)-C(12)	116.9(12)	P(1)-C(11)-C(16)	121.2(11)
C(12)-C(11)-C(16)	122.0(16)	C(11)-C(12)-C(13)	119.1(17)
C(12)-C(13)-C(14)	121.5(18)	C(13)-C(14)-C(15)	118.8(20)
C(14)-C(15)-C(16)	121.1(18)	C(11)-C(16)-C(15)	117.4(14)
P(2)-C(31)-C(32)	118.0(9)	P(2)-C(31)-C(36)	121.5(9)
C(32)-C(31)-C(36)	120.5(11)	C(31)-C(32)-C(33)	118.9(12)
C(32)-C(33)-C(34)	121.5(14)	C(33)-C(34)-C(35)	119.2(14)
C(34)-C(35)-C(36)	120.4(14)	C(31)-C(36)-C(35)	119.5(13)
P(2)-C(41)-C(42)	120.5(12)	P(2)-C(41)-C(46)	120.5(13)
C(42)-C(41)-C(46)	118.9(16)	C(41)-C(42)-C(43)	119.2(15)
C(42)-C(43)-C(44)	117.9(19)	C(43)-C(44)-C(45)	122.5(22)
C(44)-C(45)-C(46)	120.4(21)	C(41)-C(46)-C(45)	120.9(18)
P(1)-C(21)-C(26)	126.6(12)	P(1)-C(21)-C(22)	118.6(13)
C(26)-C(21)-C(22)	113.5(17)	C(21)-C(26)-C(25)	122.0(17)
C(26)-C(25)-C(24)	124.7(21)	C(25)-C(24)-C(23)	114.6(23)
C(21)-C(22)-C(23)	119.2(19)	C(24)-C(23)-C(22)	124.9(23)

3.4.3 Comparison of the Two Secondary Phosphine Complexes

As expected from the work done previously on secondary phosphine complexes of platinum(II), the dialkyphosphine complex was more stable with respect to decomposition to phosphido species and more readily prepared than the diaryl phosphine complex. The X-ray crystal structures of (3.26) and (3.31) show how both the phosphines orientate themselves in the solid state such that the P-H groups point towards each other, presumably to minimise the steric interactions of the more bulky aryl and alkyl groups.

3.5 Palladium(II) Complexes of 1,3,5,7-Tetramethyl-2,4,8-trioxa-6-Phosphaadamantane

The addition of two equivalents of the secondary phosphine (3.1) to $[\text{PdCl}_2(\text{cod})]$ in dichloromethane afforded a yellow solid. This yellow solid was characterised by $^{31}\text{P}\{^1\text{H}\}$, proton coupled ^{31}P , ^1H and $^{13}\text{C}\{^1\text{H}\}$ NMR spectroscopy (Tables 3.8 - 3.10) and elemental analysis (Experimental) and assigned the structure *trans*- $[\text{PdCl}_2(\text{adamphos})_2]$ (3.33).



$X = \text{Cl}$ (3.33)

$X = \text{Br}$ (3.34)

$X = \text{I}$ (3.35)

The $^{31}\text{P}\{^1\text{H}\}$ NMR spectrum shows two singlets with very similar chemical shifts [$\delta(^{31}\text{P})$ 3.0 p.p.m. and 2.7 p.p.m.] in approximately 1:1 ratio. The phosphine (3.1) exists in two enantiomeric forms and so these two signals were attributed to the presence of diastereomers of the palladium complex containing two of these phosphines. To a first approximation the proton coupled ^{31}P NMR spectrum is a doublet of doublets, but in fact the spin system is an AA'XX' [$|^1\text{J}(\text{PH}) + ^3\text{J}(\text{PH})|$ 368 Hz]. The *cis* platinum(II) complex (3.26) has a much smaller $^2\text{J}(\text{PP}')$ value and only a broad doublet is observed (Section 3.3). The ^1H NMR spectrum for the *trans* complex (3.33) shows a distinctive pattern in the P-H region (Figure 3.9), similar to that observed for *trans*-[PdCl₂(PH*t*Bu)₂] in the work of Shaw *et al.*¹⁰⁰

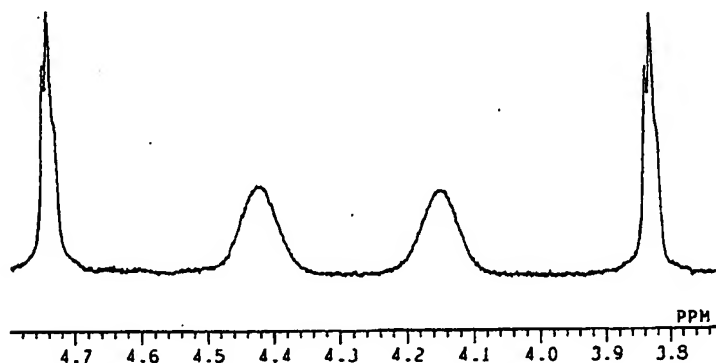


Figure 3.9 The ^1H NMR spectrum for the P-H region of the complex (3.33).

Metathesis of the *trans* dichloropalladium(II) complex (3.33) with the appropriate lithium halide afforded the *trans* dibromopalladium(II) complex (3.34) and the corresponding diiodo complex (3.35). These complexes were similarly characterised by $^{31}\text{P}\{^1\text{H}\}$, proton coupled ^{31}P , ^1H and $^{13}\text{C}\{^1\text{H}\}$ NMR spectroscopy (Tables 3.8 - 3.10) and elemental analysis (Experimental). The $^{31}\text{P}\{^1\text{H}\}$ NMR spectra of (3.34) and (3.35) show a singlet only; presumably the expected diastereomers have coincident chemical shifts.

Table 3.8 $^{31}\text{P}\{^1\text{H}\}$ NMR^a data for the palladium(II) complexes (3.33) - (3.35).

Complex		$\delta(^{31}\text{P})$	$ ^1\text{J}(\text{PH}) + ^3\text{J}(\text{PH}) $
<i>trans</i> -[PdCl ₂ (adamphos) ₂] (3.33)		3.0, 2.7 ^b	368
<i>trans</i> -[PdBr ₂ (adamphos) ₂] (3.34)		2.5	372
<i>trans</i> -[PdI ₂ (adamphos) ₂] ^c (3.35)		-1.3	364

^a Spectra (36.2 MHz) measured in CDCl₃ at 28 °C. Chemical shifts [$\delta(^{31}\text{P})$] in p.p.m. (± 0.1) to high frequency of 85% H₃PO₄. Coupling constants in Hz (± 3).

^b Two signals due to the presence of diastereomers.

^c Spectrum measured in CD₂Cl₂.

The $^{13}\text{C}\{^1\text{H}\}$ and ^1H NMR spectra for the dichloropalladium(II) complex (3.33) - (3.35) are complicated by the presence of the two diastereomers and the data are reported in Tables 3.9 and 3.10. The *trans* stereochemistry is readily assigned by virtue of the virtual triplets observed for the P-C-O carbon signals in the $^{13}\text{C}\{^1\text{H}\}$ NMR spectrum.

3.6 Some Preliminary Studies of the Reactions of 1,3,5,7-Tetramethyl-2,4,8-trioxa-6-Phosphaadamantane with Other Metals

The addition of two equivalents of the secondary phosphine (3.1) to [M₂Cl₂(cod)₂] [M = Rh; M = Ir] resulted in bridge cleavage of the dimer to afford the complexes [MCl(cod)(adamphos)] [(3.36) M = Rh; (3.37) M = Ir]. The $^{31}\text{P}\{^1\text{H}\}$ NMR spectrum of the rhodium(I) complex (3.36) shows a doublet [$^1\text{J}(\text{RhP})$ 156 Hz] and that of (3.37) shows a singlet. In both cases the proton coupled ^{31}P NMR spectrum confirms the P-H bond has remained intact on co-ordination to the metal centre. The $^{31}\text{P}\{^1\text{H}\}$ NMR data for the complexes (3.36) and (3.37) are reported in Table 3.11.

Table 3.9 ^1H NMR^a data for the palladium(II) complexes (3.33) - (3.35).

Complex	$\delta(^1\text{H})$ P-H	$ ^1J(\text{PH}) + ^3J(\text{PH}) $	$\delta(^1\text{H})$ CH_3^{b}	$\delta(^1\text{H})$ CH_3^{c}	$\delta(^1\text{H})$ CH_2^{d}
<i>trans</i> -[PdCl ₂ (adamphos) ₂] (3.33)	4.28	363	1.43, 1.39	1.68	1.97, 2.80
<i>trans</i> -[PdBr ₂ (adamphos) ₂] (3.34)	4.78	367	1.37, 1.32	1.60	1.91, 2.86
<i>trans</i> -[PdI ₂ (adamphos) ₂] (3.35)	6.13	369	1.47, 1.40	1.64	2.08, 3.07

^a Spectra (400 MHz) measured in CDCl_3 at 20 °C. Chemical shifts [$\delta(^1\text{H})$] in p.p.m. (± 0.01) to high frequency of tetramethylsilane. Coupling constants in Hz (± 0.1).

^b Two singlets observed for the two sets of methyl protons furthest away from the phosphorus.

^c A multiplet observed for the two sets of methyl protons closest to the phosphorus.

^d The four inequivalent methylene protons are observed as two distinct multiplets.

Table 3.10 $^{13}\text{C}(^1\text{H})$ NMR^a data for the palladium(II) complexes (3.33) - (3.35).

Complex	$\delta(^{13}\text{C})$ CH_3^b	$\delta(^{13}\text{C})$ CH_3^d	$\delta(^{13}\text{C})$ CH_3^d	$\delta(^{13}\text{C})$ CH_2	$\delta(^{13}\text{C})$ CH_2	$\delta(^{13}\text{C})$ P-C-Oe	$\delta(^{13}\text{C})$ P-C-Oe	$\delta(^{13}\text{C})$ O-C-Oe
<i>trans</i> -[PdCl ₂ (adamphos) ₂] (3.33)	27.4	27.3 ^c	27.6, 27.7 ^c	29.0, 28.8 ^c	39.9, 39.7 ^c	46.6, 46.6 ^c	72.2(26.0)	73.4(13.8) ^c
<i>trans</i> -[PdBr ₂ (adamphos) ₂] (3.34)	27.3	28.2, 28.3 ^c	29.0, 29.1 ^c	39.6, 39.7 ^c	46.8, 46.8 ^c	72.2(26.0) ^c	73.6(19.8)	73.6(19.8)
<i>trans</i> -[PdBr ₂ (adamphos) ₂] (3.35)	27.2	29.2	29.3	39.4	46.9	72.3(25.9)	73.7(21.3)	72.3(25.9)

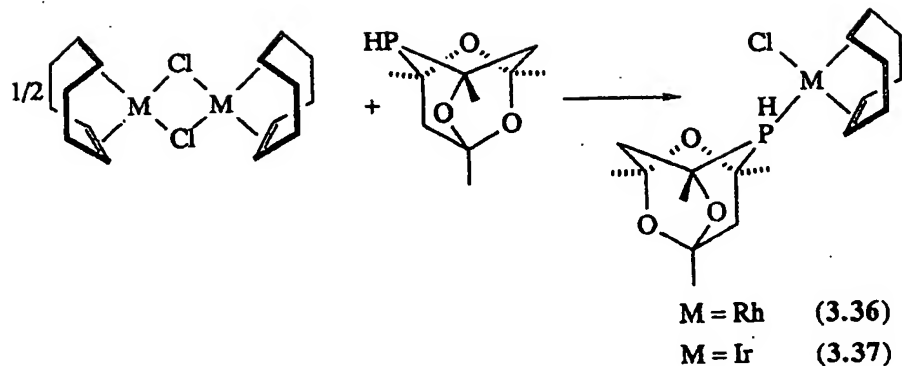
^a Spectra (100 MHz) measured in CDCl_3 at 20 °C. Chemical shifts [$\delta(^{13}\text{C})$] in p.p.m. (± 0.1) to high frequency of tetramethylsilane. Coupling constants in Hz (± 0.1).

^b The methyl carbons furthest away from the phosphorus.

^c Two signals due to the presence of diastereomers.

^d The methyl carbons closest to the phosphorus.

^e Virtual triplets; $|J(\text{PC}) + 3J(\text{PC})|$ values in parentheses.



Equation 3.9

Shaw *et al*¹⁰⁰ reported the synthesis of *trans*-[RhCl(CO)(PH*t*Bu₂)₂] from [Rh₂Cl₂(CO)₄] and four equivalents of di-*t*-butylphosphine (two equivalents per rhodium). We observed similar bridge cleavage of [Rh₂Cl₂(CO)₄] with the secondary phosphine (3.1) to afford *trans*-[RhCl(CO)(adamphos)₂] (3.38). The ³¹P{¹H} NMR spectrum shows a doublet [¹J(RhP) 117 Hz] (Table 3.11). We were not able to fully analyse the AA'MXX' pattern observed in the proton coupled ³¹P NMR spectrum (Figure 3.10).

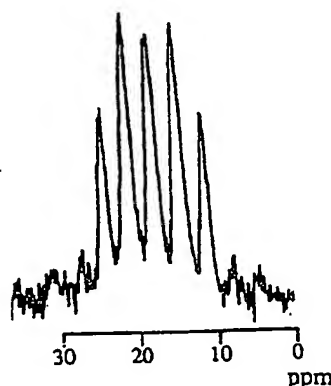


Figure 3.10 The proton coupled ³¹P NMR spectrum for the rhodium complex (3.38).

Finally the reaction of [AuCl(tht)] (tht = tetrahydrothiophene) with the secondary phosphine (3.1) afforded [AuCl(adamphos)] (3.39). The ³¹P{¹H} NMR spectrum (Table 3.11) shows a slightly broad singlet ($w_{1/2} = 14.5$ Hz) which on cooling to -60 °C shows a sharp singlet. The proton coupled ³¹P NMR spectrum at -60 °C shows a doublet confirming the P-H bond has remained intact on co-ordination to the gold(I) centre.

The complexes (3.36) - (3.39) were also characterised by elemental analysis (Experimental).

Table 3.11 $^{31}\text{P}\{^1\text{H}\}$ NMR^a data for the complexes (3.36) - (3.39).

Complex		$\delta(^{31}\text{P})^b$	$^1\text{J}(\text{PH})$
[RhCl(cod)(adamphos)]	(3.36)	13.7 (159)	327
[IrCl(cod)(adamphos)]	(3.37)	8.0	337
<i>trans</i> -[RhCl(CO)(adamphos) ₂]	(3.38)	13.8 (117)	-e
[AuCl(adamphos)] ^c	(3.39)	0.4	-
[AuCl(adamphos)] ^{c,d}	(3.39)	1.6	386

^a Spectra (36.2 MHz) measured in CDCl_3 at 28 °C. Chemical shifts [$\delta(^{31}\text{P})$] in p.p.m. (± 0.1) to high frequency of 85% H_3PO_4 . Coupling constants in Hz (± 3).

^b $^1\text{J}(\text{RhP})$ values in parentheses.

^c Spectrum measured in CD_2Cl_2 .

^d Spectrum recorded at -60 °C.

^e Due to the second order nature of the spectrum this value was not calculated.

3.7 Conclusions

The fused tricyclic secondary phosphine (3.1) forms stable complexes with a range of transition metals. It has shown no tendency to form phosphido bridged complexes. In the future it would be interesting to study the reactivity of the coordinated secondary phosphine with respect to deprotonation and hydroporphosphination reactions.